

## IDENTIFIABILITY AND ESTIMATION OF PHARMACOKINETIC PARAMETERS FOR THE LIGANDS OF THE MACROPHAGE MANNOSE RECEPTOR

NATHALIE VERDIÈRE\*, LILIANNE DENIS-VIDAL\*\*  
GHISLAINE JOLY-BLANCHARD\*, DOMINIQUE DOMURADO\*\*\*

\* Department Génie Informatique, University of Technology of Compiègne  
BP 20 529, 60 205 Compiègne Cedex, France  
e-mail: nathalie.verdiere@dma.utc.fr, ghislaine.joly-blanchard@utc.fr

\*\* University of Sciences and Tech. Lille, France  
e-mail: denvid@attglobal.net

\*\*\* CRBA — Faculty of Pharmacy  
BP 14 491, 34093 Montpellier Cedex 5, France  
e-mail: domurado@univ-montpl.fr

The aim of this paper is numerical estimation of pharmacokinetic parameters of the ligands of the macrophage mannose receptor, without knowing *a priori* the values of these parameters. However, it first requires a model identifiability analysis, which is done by applying an algorithm implemented in a symbolic computation language. It is shown that this step can lead to a direct numerical estimation algorithm. In this way, a first estimate is computed from noisy simulated observations without *a priori* parameter values. Then the resulting parameter estimate is improved by using the classical least-squares method.

**Keywords:** nonlinear systems, identifiability, parameter estimation, biological applications

### 1. Introduction

Intracellular infections are an important worldwide health problem. For instance, it is estimated that tuberculosis, caused by the facultative intracellular bacterium *Mycobacterium tuberculosis*, kills 2–3 million people each year.

Macrophage lifetime is much longer than the lifetime of granulocytes, the latter cells forming the body's first line of defense against infectious organisms. Thus, bacteria which evolved resistance against macrophage defense mechanisms can survive for a long time in the body, being protected from immune responses. Moreover, antibiotic concentrations are often lower inside cells than in extracellular fluids. Consequently, intracellular infections determine diseases difficult to cure.

Targeting anti-infectious drugs toward macrophages could bring the drugs in close contact with intracellular bacteria and thus help to fight the diseases they determine. In order to reach this goal, macromolecular carriers bearing the drug and a homing device directed toward the mannose receptor of macrophages were used (Balazuc *et al.*, 2005; Roseeuw *et al.*, 2003).

Before synthesizing macromolecular conjugates and studying their *in vivo* efficacy, it was necessary to explore the capacity of the macrophage mannose receptor to endocytose soluble macromolecules and to quantify the different aspects of such a process. Glucose oxidase, a mannosylated enzyme easily detected in biological samples through spectrophotometric, potentiometric (Aubrée-Lecat *et al.*, 1989) or immunologic techniques (de Bellefontaine *et al.*, 1994), was used for a first pharmacokinetic study of the mannose receptor activity *in vivo* (Demignot and Domurado, 1987).

After bolus intravenous administration of glucose oxidase, its pharmacokinetic behavior is represented by the following system:

$$\begin{cases} \dot{x}_1 = \alpha_1(x_2 - x_1) - \frac{V_m x_1}{k_c + x_1}, & x_1(0) = C_0, \\ \dot{x}_2 = \alpha_2(x_1 - x_2), & x_2(0) = 0, \\ y = x_1, \end{cases} \quad (1)$$

where  $x_1$  is the enzyme concentration in plasma,  $x_2$  its concentration in Compartment 2, and  $V_m$  is the maximum rate of an uptake by macrophages through the mannose receptor. The receptor-mediated uptake is a cellular

process taking place at the level of the macrophage membrane. Here  $k_c$ , the uptake constant, is the molar concentration of the ligand which produces one half of the  $V_m$  uptake. It is usually close to the affinity constant between the ligand and the receptor. Moreover,  $\alpha_1$  is the rate constant of the transfer from Compartment 1 (or the central compartment), practically plasma, to Compartment 2 (or the peripheral compartment), which represents in the model the part of the extravascular extracellular fluid accessible to glucose oxidase. Precisely, this transfer occurs through the capillary walls, more or less rapidly depending on the different permeabilities of the capillary beds in the different organs. Therefore,  $\alpha_1$  is the sum of all the transcapillary transfers in all the organs. Furthermore,  $\alpha_2$  is the rate constant of the transfer from Compartment 2 to Compartment 1. For a macromolecule such as glucose oxidase, this transfer corresponds to the return from the extracellular fluid to blood through lymphatic circulation. The ratio  $\alpha_1/\alpha_2$  of these two parameters is equal to the ratio of the volume of the peripheral compartment to the volume of the central compartment (Aubrée-Lecat *et al.*, 1993). From the equations of the system (1), it is possible to calculate the amount of a mannose receptor ligand taken up by macrophages at any given time after an intravenous injection.

In the second step, it was necessary to study *in vivo* the targeting of mannosylated polymers to be used as carriers, preferably without labeling them since radioactivity raises problems of security and macromolecular integrity, and fluorescence labeling can modify *in vivo* targeting. Consequently, glucose oxidase and mannosylated polymers were intravenously injected simultaneously and the polymer interaction with the mannose receptor was assessed through its influence on glucose oxidase pharmacokinetics (Domurado *et al.*, 1995). This competition method gives rise to the following system:

$$\left\{ \begin{array}{l} \dot{x}_1 = \alpha_1(x_2 - x_1) - \frac{k_a V_m x_1}{k_c k_a + k_c x_3 + k_a x_1}, \\ x_1(0) = C_0, \\ \dot{x}_2 = \alpha_2(x_1 - x_2), \quad x_2(0) = 0, \\ \dot{x}_3 = \beta_1(x_4 - x_3) - \frac{k_c V_m x_3}{k_c k_a + k_c x_3 + k_a x_1}, \\ x_3(0) = \gamma C_0, \\ \dot{x}_4 = \beta_2(x_3 - x_4), \quad x_4(0) = 0, \\ y = x_1. \end{array} \right. \quad (2)$$

The variables  $x_1$  and  $x_2$  are the same glucose oxidase concentrations as in the system (1). The variable  $x_3$  is the plasma concentration of the mannosylated polymer that acts as a competitor of glucose oxidase for the mannose receptor of macrophages. The variable  $x_4$  is

the concentration of the same competitor in the part of the extravascular fluid of the organs accessible to this macromolecule. Glucose oxidase and its competitor being different molecules, it should be noted that their respective second compartments are not identical.

In this system, the first two equations describe pharmacokinetic behavior of glucose oxidase whereas the third and fourth equations describe pharmacokinetic behavior of its competitor.

Being a characteristic of endocytosis by the macrophage population,  $V_m$  is the same irrespective of the ligand and is therefore identical in the first and the third equations. The uptake constant is a characteristic of the couple formed by the macrophage mannose receptor and its ligand. Consequently, we have two different constants,  $k_c$  when glucose oxidase is the ligand, and  $k_a$  for its competitor. Likewise, the transfer between compartments depends on the molecule being transferred. Therefore,  $\alpha_1$  and  $\alpha_2$  correspond to glucose oxidase and  $\beta_1$  and  $\beta_2$  to its competitor. Finally,  $\gamma$  is the ratio of the molar concentration of the polymer competitor to the molar concentration of glucose oxidase in the solution administered to the animals.

The method presented, i.e., a few animal experiments followed by numerical identification of the parameters, allows us

- to get a more rapid answer than the traditional methods (cell culture) to determine the maximum rate of uptake and the uptake constant,
- to take into account the full physiology of the animals,
- to use a minimal number of animals by fully exploiting the experimental results.

The systems (1) and (2) are nonlinear because of the hyperbolic term due to the saturability of the mannose receptor. Although the mathematics of linear pharmacokinetics has been extensively studied (Gibaldi and Perrier, 1975), it is not the case for nonlinear pharmacokinetics. In spite of the fact that only renal filtration is a linear mechanism and the reality of pharmacokinetics is otherwise nonlinear because of the saturability of many mechanisms acting on drug fate (intestinal absorption, metabolism, transfer through membrane carriers, etc.), the clinically observable pharmacokinetics of most drugs is linear because their concentration in the body is usually sufficiently small to prevent the saturation of biological processes. In mathematical terms, their therapeutic concentration is much smaller than  $k_c$ . This paper also constitutes a contribution to nonlinear pharmacokinetics.

Let us come back to numerical parameter estimation. Since the initial concentration  $C_0$  is assumed to be known, the model (1) leads to the estimation of the

parameters  $\{\alpha_1, \alpha_2, V_m, k_c\}$ , and the model (2) to the estimation of the parameters  $\{\beta_1, \beta_2, k_a, \gamma\}$ . Before performing numerical estimation, it is necessary to investigate parameter identifiability, i.e., the unique determination of the parameters from the observations. An approach to analyze model identifiability is based on differential algebra. It is outlined in Section 2.1. This approach leads to an algorithm implemented in a symbolic computation language, which is presented in Section 2.2. In the case of the model (2), there are two major difficulties: the type of nonlinearity (rational functions) and three unmeasured state variables. However, in Section 2.2, we show how the application of the algorithm yields the identifiability of both models.

Links between identifiability and numerical estimation were introduced in (Denis-Vidal *et al.*, 2003). This approach leads to a first estimate of kinetic parameters, without the knowledge of *a priori* values for these parameters, as is described in Section 3.1. Sections 3.2 and 3.3 show how the identifiability analysis leads to a first numerical estimate of the kinetic parameters of the models (1) and (2). Starting from these parameter values, the classical least-squares method produces better estimates.

The originality of the paper is principally due to the complexity of the model (2). By introducing fictitious control, the identifiability of the model obtained in such a way was proved with a local isomorphism, but it does not correspond to reality. By considering more than one experiment, it was also possible to get the identifiability of the parameters, but this requires  $V_M$  to be the same for all the experiments, which is not realistic either. A first very simplified model was studied in (Denis-Vidal *et al.*, 2003), yet the complete analysis from the identifiability proof to the numerical parameter estimation for such a complex model is completely new.

## 2. Identifiability Analysis

### 2.1. Definitions of Uncontrolled Model Identifiability

A well-known prerequisite for the well-posedness of parameter estimation is *a priori* global identifiability. Model identifiability of nonlinear systems has been extensively studied. Among the most recent and applied papers, let us cite (Denis-Vidal *et al.*, 2001a; Ljung and Glad, 1994; Vajda *et al.*, 1989).

Since the models (1) and (2) are uncontrolled, they can be described in a general state-space form as

$$\Gamma^\theta \begin{cases} \dot{x}(t, \theta) = f(x(t, \theta), \theta), & x(0, \theta) = x_0(\theta), \\ y(t, \theta) = h(x(t, \theta), \theta). \end{cases} \quad (3)$$

Here  $x(t, \theta) \in \mathbb{R}^n$  and  $y(t, \theta) \in \mathbb{R}$  denote the state variables and the measured outputs, respectively, and  $\theta \in \mathcal{U}_p$

the unknown parameters ( $\mathcal{U}_p$  is an open subset in  $\mathbb{R}^p$ ). The functions  $f(\cdot, \theta)$  and  $h(\cdot, \theta)$  are real, rational and analytic for every  $\theta \in \mathcal{U}_p$  on  $M$  (a connected open subset of  $\mathbb{R}^n$  such that  $x(t, \theta) \in M$  for every  $\theta \in \mathcal{U}_p$  and every  $t \in [0, T]$ ). Moreover, we assume that  $f(x_0(\theta), \theta) \neq 0$  for every  $\theta \in \mathcal{U}_p$ . In this paper, the identifiability definitions considered take into account initial conditions.

**Definition 1.** The model  $\Gamma^\theta$  is *globally identifiable* at  $\theta \in \mathcal{U}_p$  if there exists a finite time  $t_1 > 0$  such that if  $y(t, \tilde{\theta}) = y(t, \theta)$  ( $\tilde{\theta} \in \mathcal{U}_p$ ) for all  $t \in [0, t_1]$ , then  $\tilde{\theta} = \theta$ . The model  $\Gamma^\theta$  is *locally identifiable* at  $\theta \in \mathcal{U}_p$  if there exists an open neighborhood  $W$  of  $\theta$  such that  $\Gamma^\theta$  is globally identifiable at  $\theta$  with  $\mathcal{U}_p$  restricted to  $W$ .

In most models there exist atypical points in  $\mathcal{U}_p$  where the model is not globally (locally) identifiable. Thus, the previous definitions should be generically extended so that the model  $\Gamma^\theta$  is said to be *globally (locally) structurally identifiable* if it is globally (locally) identifiable at all  $\theta \in \mathcal{U}_p$  except at the points of a subset of measure zero in  $\mathcal{U}_p$ . Sometimes, identifiability results are obtained independently of the initial conditions. Thus, if  $x(0, \theta) = x_0(\theta)$  is removed from  $\Gamma^\theta$ , it gives  $\Sigma^\theta$ :

$$\Sigma^\theta \begin{cases} \dot{x}(t, \theta) = f(x(t, \theta), \theta), \\ y(t, \theta) = h(x(t, \theta), \theta). \end{cases} \quad (4)$$

Then the solutions of  $\Sigma^\theta$  may be nonunique and some solutions might be of a degenerate character. Thus, the set of nondegenerate solutions will be denoted by  $\bar{x}(\theta)$ , the set of corresponding outputs by  $\bar{y}(\theta)$  and the definition introduced in (Ljung and Glad, 1994) is adopted here:

**Definition 2.** The model  $\Sigma^\theta$  is *globally identifiable* at  $\theta \in \mathcal{U}_p$  if for any  $\tilde{\theta} \in \mathcal{U}_p$ ,  $\tilde{\theta} \neq \theta$ ,  $\bar{y}(\theta) \neq \emptyset$  and  $\bar{y}(\theta) \cap \bar{y}(\tilde{\theta}) = \emptyset$ .

Then the definitions of local (structural) identifiability are deduced in a straightforward manner.

### 2.2. Identifiability Algorithm

The identifiability approach adopted here is based on the differential algebra, which is possible since  $f(\cdot, \theta)$  and  $h(\cdot, \theta)$  are assumed to be rational functions. It consists in eliminating unobservable state variables in order to get relations between outputs and parameters. It is not obvious how to do such a computation only with a pencil and paper, but there exist software environments equipped with symbolic computation languages (Denis-Vidal *et al.*, 2001b; Ljung and Glad, 1994).

More precisely, the system  $\Sigma^\theta$  is rewritten as a differential polynomial system, complemented with  $\dot{\theta}_i =$

0,  $i = 1, \dots, p$ . The resulting system can be described by the following polynomial equations and inequalities:

$$\begin{cases} p(\dot{x}, x, \theta) = 0, \\ q(x, y, \theta) = 0, \\ r(x, y, \theta) \neq 0, \\ \dot{\theta}_i = 0, \quad i = 1, \dots, p. \end{cases} \quad (5)$$

A solution of  $\Sigma^\theta$  is any triplet  $\{x, y, \theta\}$  satisfying (5).

Before presenting our identifiability algorithm, let us recall some notation and some subsidiary results (Denis-Vidal et al., 2001b):

- $\mathcal{I}$  is the radical of the differential ideal generated by (5).  $\mathcal{I}$ , endowed with the following ranking which eliminates the state variables:

$$[\theta] \prec [y] \prec [x], \quad (6)$$

is assumed to admit a characteristic presentation (i.e., a canonical representant of the ideal). It is shown that this characteristic presentation, evaluated at  $\theta$ , has the following form:

$$\mathcal{C}(\theta) = \{\dot{\theta}_1, \dots, \dot{\theta}_p, P(y, \theta), Q_1(x, y, \theta), \dots, Q_n(x, y, \theta)\}.$$

- $\mathcal{I}_\theta^o$  is the ideal obtained after eliminating state variables. Then it is necessary to make some “technical assumptions” about the polynomials of  $\mathcal{C}(\theta)$  (Denis-Vidal et al., 2001b), which is explained in Appendix. In this way, the characteristic presentation  $\mathcal{C}_\theta^o$  of  $\mathcal{I}_\theta^o$ , called the *output characteristic presentation*, is proved to contain the differential polynomial  $P(y, \theta)$ , called the *output polynomial*, which can be expressed as

$$P(y, \theta) = \sum_{i=1}^l g_i(\theta)\phi_i(y) + \phi_{l+1}(y), \quad (7)$$

where  $(g_i(\theta))_{1 \leq i \leq l}$  are rational in  $\theta$ ,  $g_i \neq g_j$  ( $i \neq j$ ),  $(\phi_i)_{1 \leq i \leq l}$  are differential polynomials with respect to  $y$ , and  $\phi_{l+1} \neq 0$ . The list

$$\{g_1(\theta), g_2(\theta), \dots, g_l(\theta)\} \quad (8)$$

is called the *exhaustive summary*.

The identifiability algorithm is based on the following proposition (Denis-Vidal et al., 2001a):

**Proposition 1.** *Set*

$$\Delta P(y) = \det(\phi_i(y), i = 1, \dots, l + 1). \quad (9)$$

If  $\Delta P(y)$  is not in  $\mathcal{I}_\theta^o$ , then  $\Sigma^\theta$  is globally identifiable at  $\theta$  if and only if for every  $\bar{\theta} \in \mathcal{U}_p$  ( $\bar{\theta} \neq \theta$ ), the two characteristic presentations  $\mathcal{C}_\theta^o$  and  $\mathcal{C}_{\bar{\theta}}^o$  are distinct.

The algorithm, elaborated by ourselves, is written in MAPLE 7. The second and fifth steps are based on the Rosenfeld-Groebner algorithm, which was implemented by Boulier in MAPLE 7 (Boulier et al., 1995), and is available in the DIFFALG package.

**Data:**  $f$  and  $h$  (the functions occurring in  $\Sigma^\theta$ ).

**Step 1:** Software rewrites the original system  $\Sigma^\theta$  (4) as the differential polynomial system (5).

**Step 2:** The Rosenfeld-Groebner algorithm computes the general input-output characteristic presentation. (If the user is interested by all the input-output characteristic presentations involving all the particular cases, he or she can require them.)

**Step 3:** The software computes the values of  $\theta$  such that the “technical assumptions” (given in the Appendix) about the polynomials of  $\mathcal{C}(\theta)$  are not valid.

**Step 4:** It saves the coefficients  $\{g_i(\theta), i = 1, \dots, l\}$  in an exhaustive summary, which is simplified in order to extract its smallest generator system in terms of the degree, the number of monomials, etc.

**Step 5:** The exhaustive summary is analyzed by the Rosenfeld-Groebner algorithm that solves

$$\begin{cases} g_i(\theta) = g_i(\bar{\theta}), & i = 1, \dots, l, \\ \dot{\theta}_i = 0, & i = 1, \dots, p. \end{cases} \quad (10)$$

**Step 6:** The software validates the method by checking the assumption of Proposition 1. Let us note that, if the assumption is valid, then the solutions are not degenerate.

In this section, the identifiability of the model is analyzed without considering initial conditions. But the results or Proposition 1 could be improved by adding information from such conditions.

### 2.3. Application to Pharmacokinetics

Firstly, the algorithm is applied to the model (1) with  $\theta = \{\alpha_1, \alpha_2, V_m, k_c\}$ . The successive steps give the following results:

*Step 1:* The software rewrites the system as the following polynomial differential system:

$$\begin{cases} \dot{x}_1(k_c + x_1) - \alpha_1(x_2 - x_1)(k_c + x_1) + (V_m x_1) = 0, \\ \dot{x}_2 - \alpha_2(x_1 - x_2) = 0, \\ y - x_1 = 0, \\ k_c + x_1 \neq 0, \\ \dot{\alpha}_1 = 0, \quad \dot{\alpha}_2 = 0, \quad \dot{V}_m = 0, \quad \dot{k}_c = 0. \end{cases} \quad (11)$$

*Step 2:* It returns the following general output characteristic presentation with the assumption that  $\alpha_1 \neq 0$ :

$$\{2k_c\ddot{y}y + k_c^2\dot{y} + (\alpha_1 + \alpha_2)\dot{y}y^2 + 2k_c(\alpha_1 + \alpha_2)\dot{y}y + ((\alpha_1 + \alpha_2)k_c + V_m)k_c\dot{y} + \alpha_2V_my^2 + \alpha_2V_mk_cy - \dot{y}y^2\}. \quad (12)$$

(The particular case of  $\alpha_1 = 0$  does not correspond to any realistic assumption.)

*Step 3:* The “technical assumptions” about the polynomials of  $\mathcal{C}(\theta)$  are not valid if  $V_mk_c = 0$  (see Appendix). Consequently, the set  $\mathcal{U}_p$  is defined by  $\mathcal{U}_p = \{\theta \in \mathbb{R}^4, \alpha_1 \neq 0, V_mk_c \neq 0\}$ .

*Step 4:* The exhaustive summary, given by the software, is

$$\{k_c\alpha_2V_m, k_c^2, k_c, k_c(\alpha_1 + \alpha_2), \alpha_2V_m, \alpha_1 + \alpha_2, k_c(k_c\alpha_2 + k_c\alpha_1 + V_m)\}. \quad (13)$$

*Step 5:* The analysis of this exhaustive summary leads to

$$\{V_m = \bar{V}_m, k_c = \bar{k}_c, \alpha_1 = \bar{\alpha}_1, \alpha_2 = \bar{\alpha}_2\}. \quad (14)$$

*Step 6:* It verifies that

$$\det\{\ddot{y}y, \dot{y}, \dot{y}y^2, \dot{y}y, \dot{y}, y^2, y\} \text{ is not in } \mathcal{I}_\theta^0.$$

All these steps show that the model (1) is globally identifiable with respect to  $\mathcal{U}_p$  or structurally globally identifiable with respect to  $\mathbb{R}^4$ .

Now, the software applied to the model (2) does not imply anything because the computations require too much memory. But it is possible to give more information to the software. Indeed, the state  $x_2$  can be considered as a new observed state because it is known as the unique solution of

$$\dot{x}_2 + \alpha_2x_2 = \alpha_2y, \quad x_2(0) = 0. \quad (15)$$

On the other hand, from the first equation of (2), we have

$$\dot{x}_1 = \alpha_1(x_2 - x_1) - \frac{V_m}{k_c} \frac{x_1}{1 + x_3/k_a + x_1/k_c}. \quad (16)$$

The quantity  $x_3/k_a$  can be considered as known. Consequently, the quantity

$$\frac{x_3/k_a}{1 + x_3/k_a + x_1/k_c}$$

is known, too. Therefore the algorithm is applied to the model (2) with

$$y = \left(x_1, x_2, \frac{x_3/k_a}{1 + x_3/k_a + x_1/k_c}, \frac{x_3}{k_a}\right)$$

and

$$\theta = \{\beta_1, \beta_2, k_a\}.$$

*Step 1:* The software rewrites the system as the following polynomial differential system:

$$\begin{cases} \dot{x}_1(k_ck_a + k_cx_3 + k_ax_1) - \alpha_1(x_2 - x_1) \\ \quad \times (k_ck_a + k_cx_3 + k_ax_1) + k_aV_mx_1 = 0, \\ \dot{x}_2 - \alpha_2(x_1 - x_2) = 0, \\ \dot{x}_3(k_ck_a + k_cx_3 + k_ax_1) - \beta_1(x_4 - x_3) \\ \quad \times (k_ck_a + k_cx_3 + k_ax_1) + k_cV_mx_3 = 0, \\ \dot{x}_4 - \beta_2(x_3 - x_4) = 0, \\ y_1 - x_1 = 0, \\ y_2 - x_2 = 0, \\ y_3(k_ak_c + k_cx_3 + k_ax_1) - k_cx_3 = 0, \\ k_ay_4 - x_3 = 0, \\ k_ck_a + k_cx_3 + k_ax_1 \neq 0 \\ \dot{\beta}_1 = 0, \quad \dot{\beta}_2 = 0, \quad \dot{k}_a = 0. \end{cases} \quad (17)$$

*Step 2:* It returns the following general output characteristic presentation:

$$\begin{aligned} &\left\{ \ddot{y}_4y_4^2k_ck_a + \dot{y}_4y_4^2k_c(\beta_1 + \beta_2)k_a + y_4^2y_3k_cV_m\beta_2 \right. \\ &\quad - (y_3^3y_4 - y_3^2y_4 + y_3^3)V_m^2 - (-y_3y_4\dot{y}_4 - y_3^2y_4\dot{y}_4)k_cV_m \\ &\quad - \left( \frac{y_2^2y_4^2}{k_c} - y_3y_4^2 + \frac{y_2^2}{k_c}y_3^2y_4 + y_3^2y_4 \right) \alpha_1k_cV_m, \\ &\quad (\dot{y}_3y_4^2 + y_3y_4\dot{y}_4 + y_3^2y_4\dot{y}_4)k_c + (y_3^3y_4 - y_3^2y_4 + y_3^3)V_m \\ &\quad + \left( \frac{y_2^2}{k_c}y_3^2y_4 + y_3^2y_4 + y_3^2y_4^2 - y_3y_4^2 \right) \alpha_1k_c, \\ &\quad y_1y_3 + (y_3 + y_3y_4 - y_4)k_c, \\ &\quad \left. \dot{y}_2y_3 + y_2y_3\alpha_2 + (y_3 - y_3y_4 + y_4)\alpha_2k_c \right\}. \end{aligned}$$

Only the first polynomial involves the unknown parameters. The other polynomials correspond to the known relations between the “artificial” outputs introduced in order to simplify the computation of the characteristic presentation. (The particular cases  $\beta_1 = 0$  and  $x_3 = 0$  are not considered).

*Step 3:* The “technical assumptions” about the polynomials of  $\mathcal{C}(\theta)$  are not valid if  $k_a = 0$ . Consequently, the set  $\mathcal{U}_p$  is defined by  $\mathcal{U}_p = \{\theta \in \mathbb{R}^3, k_a \neq 0\}$ .

*Step 4:* The exhaustive summary, given by the software, can be expressed as

$$\{k_a, \beta_2, k_a(\beta_1 + \beta_2)\}. \quad (18)$$

*Step 5:* The analysis of this exhaustive summary leads to

$$\{k_a = \bar{k}_a, \beta_1 = \bar{\beta}_1, \beta_2 = \bar{\beta}_2\}. \quad (19)$$

*Step 6:* It verifies that  $\det\{\ddot{y}_4, \dot{y}_4, y_3\}$  is not in  $\mathcal{I}_\theta^0$ .

All these steps show the model (2) (without initial conditions) to be globally identifiable at  $\theta = \{\beta_1, \beta_2, k_a\}$  with respect to  $\mathcal{U}_p$  or structurally globally identifiable with respect to  $\mathbb{R}^3$ . As regards the parameter  $\gamma$  involved only in the initial condition, its uniqueness can be directly deduced from the first equation at the time  $t = 0$ , i.e.,

$$\dot{y}_1(0) = -\alpha_1 C_0 - \frac{k_a V_m C_0}{k_c k_a + k_c \gamma C_0 + k_a C_0}.$$

### 3. Preliminary Numerical Parameter Estimation

#### 3.1. Idea

In the previous section, only one output polynomial gives information about model identifiability. It can be written down as

$$\sum_{i=1}^l g_i(\theta) \phi_i(y) + \phi_{l+1}(y) = 0. \quad (20)$$

Since initial conditions play a role in the identifiability procedure, a way of considering these conditions is the integration of the relations (20) from 0 to  $t$ . The aim of this computation is not only to facilitate identifiability analysis by the introduction of initial conditions, but also to reduce the highest order of the time derivative, which is a source of numerical instabilities.

The integration will be performed as far as possible and the resulting relations will be called the integro-differential equation of observation:

$$T(y, \theta) = 0. \quad (21)$$

Since (21) can be obtained by integrating (20), and (20) is linear with respect to some parameter combinations,  $T(y, \theta)$  is also linear with respect to some parameter combinations. The introduction of initial conditions can give additional combinations, and  $\{\gamma_1(\theta), \dots, \gamma_l(\theta)\}$  denote the parameter combinations appearing in  $T(y, \theta)$ .

The *exact* observation, corresponding to the *exact* value  $\bar{\theta}$ , is more or less perturbed by noise. Thus, Eqns. (20) and (21) are not satisfied by the noisy output. Moreover, the observation is not carried out at any time and the given data are a set of measurements:

$$z_j := y(t_j; \bar{\theta}) + \varepsilon_j, \quad j = 1, 2, \dots, q. \quad (22)$$

The aim of this section is to provide a first estimate of the parameters directly from (21). In most cases, output derivatives are involved in (21), and they have to be estimated from noisy observations. Generally, the numerical approximation of a derivative is sensitive to noise, especially if the derivative order is high. Moreover, it is not

accurate near the bounds of the observation horizon. That is why, on the one hand, the output polynomial was integrated, and on the other hand, over a time interval away from 0. Various methods were tested in order to approximate these derivatives at the points  $(t_j)$ . Firstly, a local approximation polynomial was used, then an algorithm based on B-splines was applied (Ibrir and Diop, 2004). These do not require any knowledge of the statistics of measurement uncertainties. For our first application, they give similar results, but for the second one, the method given in (Ibrir and Diop, 2004) is better and was successfully applied.

Consider the derivatives to be estimated at  $\{t_{n_0}, \dots, t_{n_1}\}$  and denote by  $\{T_{\text{int}}(z_j, \theta)\}_{n_0 \leq j \leq n_1}$  the values of the function corresponding to the approximation of (21), in which integrals and derivatives have been numerically approximated. A way of getting an estimate of  $\{\gamma_1(\theta), \dots, \gamma_l(\theta)\}$  is to solve the following minimization problem:

$$\min_{(\gamma_1(\theta), \dots, \gamma_l(\theta))} \sum_{j=n_0}^{n_1} (T_{\text{int}}(z_j, \theta))^2. \quad (23)$$

Since the integral-differential expression  $\mathcal{T}$  is linear with respect to  $\{\gamma_1(\theta), \dots, \gamma_l(\theta)\}$ , it is the same for the function  $T_{\text{int}}$ . Therefore, the QR algorithm can be applied to solve (23). Moreover, since model identifiability has been shown, unique parameter values  $\theta$  are drawn from  $\{\gamma_1(\theta), \dots, \gamma_l(\theta)\}$ .

#### 3.2. Application to the Model (1)

The output polynomial (12) can be rewritten as

$$\ddot{y}y^2 + 2\gamma_1(\theta)\dot{y}y + \gamma_2(\theta)\ddot{y} + \gamma_3(\theta)\dot{y}y^2 + 2\gamma_4(\theta)y\dot{y} + \gamma_5(\theta)\dot{y} + \gamma_6(\theta)y^2 + \gamma_7(\theta)y = 0, \quad (24)$$

where

$$\theta = \{\alpha_1, \alpha_2, V_m, k_c\}$$

and

$$\gamma(\theta) = \{k_c, k_c^2, \alpha_1 + \alpha_2, k_c(\alpha_1 + \alpha_2), (k_c(\alpha_1 + \alpha_2) + V_m)k_c, \alpha_2 V_m, \alpha_2 V_m k_c\}.$$

The integration between  $t_0 > 0$  and  $t$  leads to

$$\begin{aligned} & \dot{y}(t)y(t)^2 - \dot{y}(t_0)y(t_0)^2 - 2 \int_{t_0}^t y(s)\dot{y}(s)^2 ds \\ & + 2\gamma_1 \left( \dot{y}(t)y(t) - \dot{y}(t_0)y(t_0) - \int_{t_0}^t \dot{y}(s)^2 ds \right) \\ & + \frac{1}{3}\gamma_2 (\dot{y}(t) - \dot{y}(t_0)) + \gamma_3 (y(t)^3 - y(t_0)^3) \\ & + \gamma_4 (y(t)^2 - y(t_0)^2) + \gamma_5 (y(t) - y(t_0)) \\ & + \gamma_6 \int_{t_0}^t y(s)^2 ds + \gamma_7 \int_{t_0}^t y(s) ds = 0. \end{aligned}$$

The integrals involved are approximated by a trapezoidal rule, which gives the following least-squares problem ( $t_0 = t_{n_0}$ ,  $t = t_k$ ,  $k = n_0, \dots, n_1$ , after discretizing in time):

$$\min_{(\gamma_1(\theta), \dots, \gamma_7(\theta))} \sum_{k=n_0}^{n_1} \left( \sum_{j=1}^7 A_{k,j} \gamma_j(\theta) - b_k \right)^2,$$

where

$$\begin{aligned} A_{k,1} &= 2(y_p(t_{n_0})y(t_{n_0}) - y_p(t_k)y(t_k)) \\ &\quad + \sum_{i=n_0}^{k-1} (t_{i+1} - t_i)(y_p(t_i)^2 + y_p(t_{i+1})^2), \\ A_{k,2} &= y_p(t_{n_0}) - y_p(t_k), \\ A_{k,3} &= \frac{1}{3}(y(t_{n_0})^3 - y(t_k)^3), \\ A_{k,4} &= (y(t_{n_0})^2 - y(t_k)^2), \\ A_{k,5} &= y(t_{n_0}) - y(t_k), \\ A_{k,6} &= -\frac{1}{2} \sum_{i=n_0}^{k-1} (t_{i+1} - t_i)(y(t_i)^2 + y(t_{i+1})^2), \\ A_{k,7} &= -\frac{1}{2} \sum_{i=n_0}^{k-1} (t_{i+1} - t_i)(y(t_i) + y(t_{i+1})), \\ b_k &= y_p(t_k)y(t_k)^2 - y_p(t_{n_0})y(t_{n_0})^2 \\ &\quad - \sum_{i=n_0}^{k-1} (t_{i+1} - t_i)(y(t_i)y_p^2(t_i) \\ &\quad + y(t_{i+1})y_p^2(t_{i+1})), \end{aligned} \quad (25)$$

and  $y_p(t_i)$  is a numerical approximation to  $\dot{y}(t_i)$ . In order to test the method, the measured state is simulated from the true signal  $\bar{y}$  computed with  $\theta = \{0.011, 0.02, 0.1, 1\}$  and disturbed by noise, so it is a random variable with the mean  $\bar{y}$  and the variance  $(\sigma\bar{y})^2$ . The coefficient  $\sigma$  is computed so that the relative error has a maximum value of 0.01 (resp. 0.05) with an error probability less than 0.003. It will be denoted by  $\sigma_1$  (resp.  $\sigma_2$ ).

If the measured data are simulated with the coefficient  $\sigma_1$  (resp.  $\sigma_2$ ), the previous least-squares minimization solved by the QR algorithm leads to the estimate  $\theta_{\sigma_1} = [0.0759, 0.0164, 0.0811, 0.1431]$  (resp.  $\theta_{\sigma_2} = [0.0343, 0.0069, 0.0759, 0.1151]$ ). Figure 1 (resp. Fig. 2) represents the measured data (dashed line), and the output (solid line) computed from the model (1) and the parameter value  $\theta_{\sigma_1}$  (resp.  $\theta_{\sigma_2}$ ).

Obviously, the results are not satisfactory, but the aim of the method is to provide a preliminary estimate of the parameters. It is used as a starting point of an iterative minimization procedure: the well-known Levenberg-Marquard algorithm. The results are very

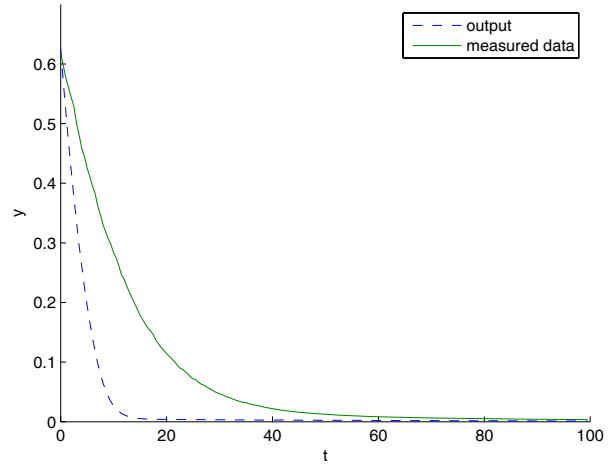


Fig. 1. System (1), noise level  $\sigma_1$ , first estimate.

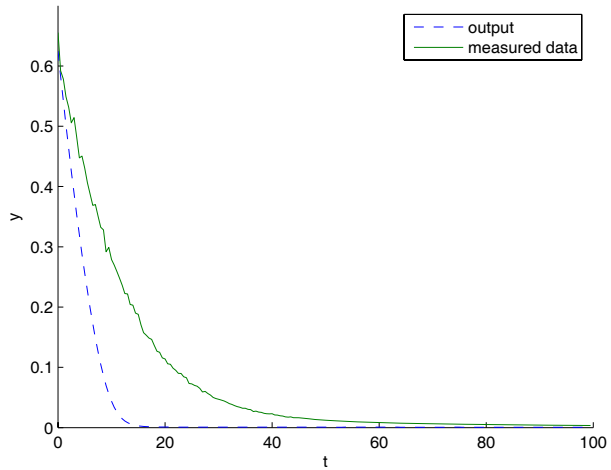


Fig. 2. System (1), noise level  $\sigma_2$ , first estimate.

satisfactory. Indeed, if the measured data are simulated with the variance  $\sigma_1$  (resp.  $\sigma_2$ ), the resulting parameter values are  $\{0.0109, 0.0196, 0.102, 1.0271\}$  (resp.  $\{0.0106, 0.0196, 0.1044, 1.0535\}$ ), which corresponds to Fig. 3 (resp. Fig. 4).

**Remark 1.** An alternative approach for estimating the parameter vector  $\theta$  from (24) could be given by an adaptive observer as is done in (Marino and Tomei, 1995). However, the above-mentioned drawbacks of the approximation of derivatives from noisy measurements seem to remain.

### 3.3. Application to the Model (2)

The previous estimation of the parameters  $(\alpha_1, \alpha_2, V_m, k_c)$  is taken into account in the model (2).

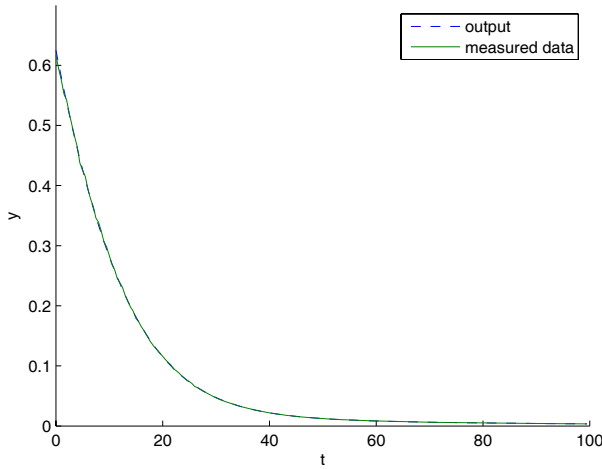


Fig. 3. System (1), noise level  $\sigma_1$ , final estimate.

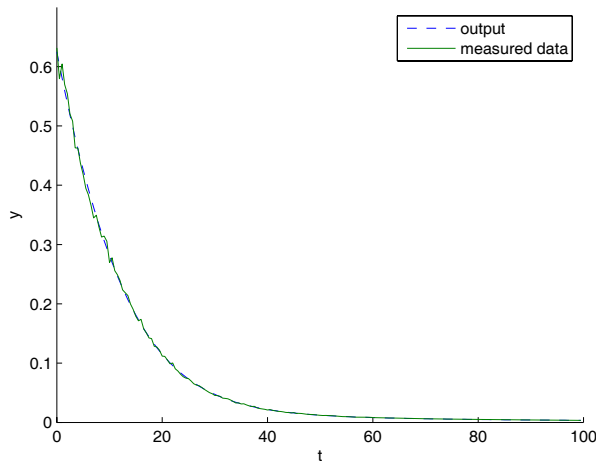


Fig. 4. System (1), noise level  $\sigma_2$ , final estimate.

In Section 2.3 the identifiability of the model (2) is given by the first polynomial of the characteristic presentation. The second polynomial permits a simplification which leads to

$$\dot{y}_4 + (\beta_1 + \beta_2)\dot{y}_4 + \frac{V_m}{k_a}\dot{y}_3 + \frac{\beta_2 V_m}{k_a}y_3 = 0. \quad (26)$$

In order to decrease the derivation order, let us integrate (26) between  $t_0$  and  $t$ :

$$\begin{aligned} & \dot{y}_4(t) - \dot{y}_4(t_0) + (\beta_1 + \beta_2)(y_4(t) - y_4(t_0)) \\ & + \frac{V_m}{k_a}(y_3(t) - y_3(t_0)) + \frac{\beta_2 V_m}{k_a} \int_{t_0}^t y_3(\tau) d\tau = 0. \end{aligned} \quad (27)$$

The corresponding least-squares problem can be expressed as

$$\min_{\theta \in \mathbb{R}^3} \|A\theta - b\|^2, \quad (28)$$

where

$$\theta = \left\{ \beta_1 + \beta_2, \frac{V_m}{k_a}, \frac{\beta_2 V_m}{k_a} \right\},$$

$$A_j = \left[ y_4(t_j) - y_4(t_0), y_3(t_j) - y_3(t_0), \int_{t_0}^{t_j} y_3(\tau) d\tau \right],$$

$$b_j = -(y_{4p}(t_j) - y_{4p}(t_0)).$$

The integral is approximated by a trapezoidal rule and  $y_{4p}(t_j)$  corresponds to a numerical estimate of  $\dot{y}_4(t_j)$ .

In order to test the method, the measured state is simulated from the true signal  $\bar{y}$  ( $C_0 = 0.625$ ) computed with  $\beta_1 = 0.01$ ,  $\beta_2 = 0.02$ ,  $k_a = 0.5$ ,  $\gamma = 50$  and disturbed by noise so that it can be treated as a random variable with the mean  $\bar{y}$  and the variance  $(\sigma\bar{y})^2$ . The coefficient  $\sigma$  is computed so that the relative error has a maximum value of 0.01 (resp. 0.05) with an error probability less than 0.003. As has been done previously, it will be denoted by  $\sigma_1$  (resp.  $\sigma_2$ ).

Then, the least-squares problem is solved using the QR algorithm, which gives the preliminary estimates  $\beta_1 = 0.0244$ ,  $\beta_2 = 0.0263$ ,  $k_a = 0.7$  (resp.  $\beta_1 = 0.017$ ,  $\beta_2 = 0.011$ ,  $k_a = 0.3$ ). The parameter  $\gamma$  is estimated from the evaluation of the first equation of (2) at  $t = 0$ :

$$\gamma = -k_a \left( \left( \frac{1}{C_0} + \frac{1}{k_c} \right) + \frac{V_m/k_c}{\dot{y}(0) + \alpha_1 C_0} \right). \quad (29)$$

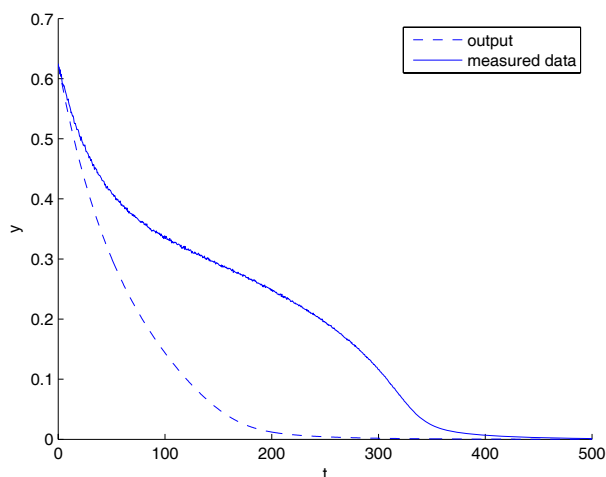
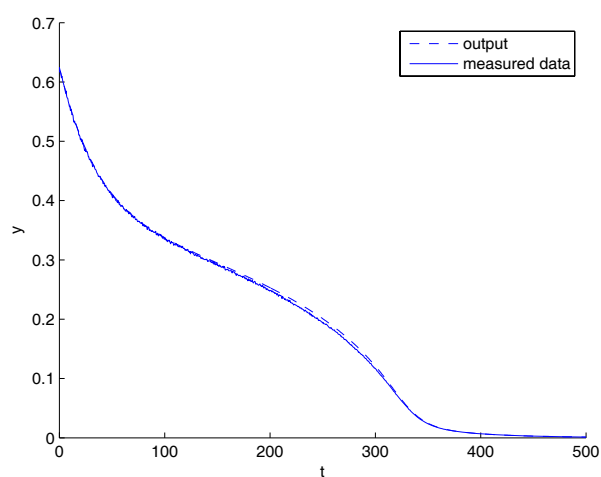
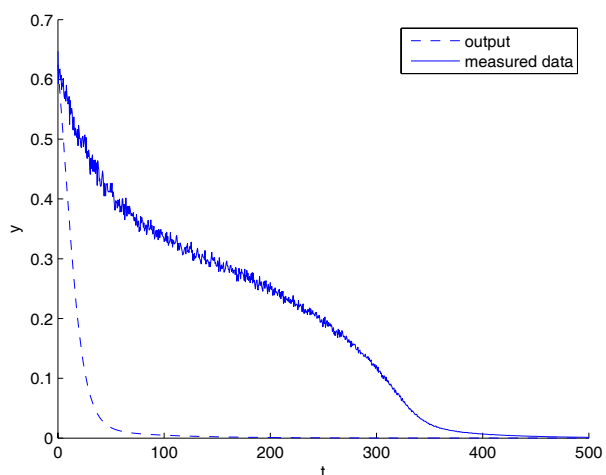
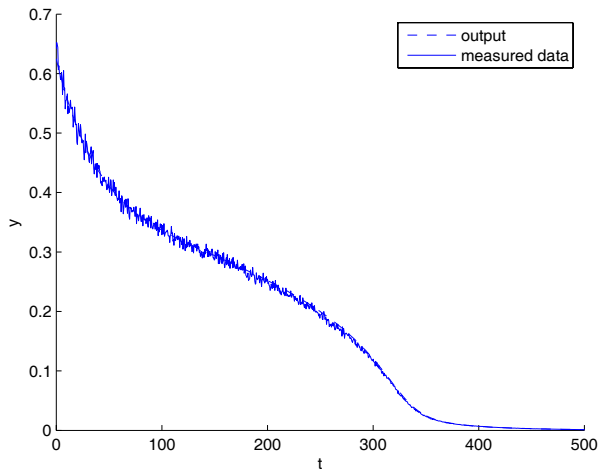
In this way,  $\gamma = 22.7376$  (resp.  $\gamma = 0.9641$ ) was found.

The parameter  $\gamma$  is estimated from the relation (29), which depends on the derivative of the observation at 0 and the estimate of  $k_a$ . It is well known that it is quite difficult to approximate values at initial conditions, especially with disturbed data. Thus the accumulation of errors makes the estimate of  $\gamma$  too bad. Figure 5 (resp. Fig. 6) represents the measured data (dashed line), and the output (solid line) computed from the model (2) and the second estimate of the parameters. The big difference between both the curves is due to the important sensitivity of the output with respect to  $\gamma$ .

As in Section 3.3, the Levenberg-Marquard algorithm is applied and the obtained parameter values of the model (2) are  $\{\beta_1, \beta_2, k_a, \gamma\} = \{0.03; 0.03; 0.29; 49.67\}$  (resp.  $\{\beta_1, \beta_2, k_a, \gamma\} = \{0.0374; 0.0328; 0.2711; 49.66\}$ ) which corresponds to Fig. 7 (resp. Fig. 8).

#### 4. Conclusion

In order to study the feasibility of antibiotic targeting toward the macrophages for the treatment of intracellular infections, we used a model macromolecule, namely, glucose oxidase, and analyzed its pharmacokinetics, which gave rise to the first system. In the second step, we used

Fig. 5. System (2), noise level  $\sigma_1$ , first estimate.Fig. 7. System (2), noise level  $\sigma_1$ , final estimate.Fig. 6. System (2), noise level  $\sigma_2$ , first estimate.Fig. 8. System (2), noise level  $\sigma_2$ , final estimate.

glucose oxidase as the sensor in a competition test designed to assess the capacity of macromolecular potential drug carriers to reach *in vivo* the macrophages. This experimental setup gave rise to the second system. Model identifiability analysis of both systems was shown by using software based on differential algebra tools. Then it was shown that this analysis leads to a differential polynomial linking some parameter combinations and system outputs, which can be used to give a preliminary numerical parameter estimate. This step does not require any information about the parameters. Lastly, starting from these parameter values, a classical least-squares problem leads to a very good numerical estimation.

## References

- Aubrée-Lecat A., Hervagault C., Delacour C., Beaudé C., Bourdillon C. and Rémy M.H. (1989): *Direct electrochemical determination of glucose oxidase in biological samples.* — Anal. Biochem., Vol. 178, No. 2, pp. 427–430.
- Aubrée-Lecat A., Duban M.C., Demignot S., Domurado M., Fournié P. and Domurado D. (1993): *Influence of barrier-crossing limitations on the amount of macromolecular drug taken up by its target.* — J. Pharmacokin. Biopharm., Vol. 21, No. 1, pp. 75–98.
- Balazuc A.-M., Lagranderie M., Chavarot P., Pescher P., Roseeuw E., Schacht E., Domurado D. and Marchal G. (2005): *In vivo efficiency of targeted norfloxacin against persistent, isoniazid-insensitive, Mycobacterium bovis BCG present in the physiologically hypoxic mouse liver.* — Microbes Infect., Vol. 7, No. 7–8, pp. 969–975.
- Boulier F., Lazard D., Ollivier F. and Petitot M. (1995): *Representation for the radical of a finitely generated differential ideal.* — Proc. Int. Symp. Symbolic and Algebraic Computation, ISSAC'95, Montréal, Canada, pp. 158–166.
- de Bellefontaine C., Josse F., Domurado M. and Domurado D. (1994): *Immunoassay for native enzyme quantification in biological samples.* — Appl. Biochem. Biotech., Vol. 48, No. 2, pp. 117–123.

Demignot S., and Domurado D. (1987): *Effect of prosthetic sugar groups on the pharmacokinetics of glucose-oxidase.* — Drug Design Deliv., Vol. 1, No. 4, pp. 333–348.

Denis-Vidal L., Joly-Blanchard G. and Noiret C. (2001a): *Some effective approaches to check the identifiability of uncontrolled nonlinear systems.* — Math. Comp. Simul., Vol. 57, No. 1, pp. 35–44.

Denis-Vidal L., Joly-Blanchard G., Noiret C., and Petitot M. (2001b): *An algorithm to test identifiability of non-linear systems.* — Proc. 5th IFAC Conf. Nonlinear Control Systems, NOLCOS, St. Petersburg, Russia, pp. 174–178.

Denis-Vidal L., Joly-Blanchard G. and Noiret C. (2003): *System identifiability (symbolic computation) and parameter estimation (numerical computation).* — Numer. Algo., Vol. 34, No. 2–4, pp. 282–292.

Domurado M., Domurado D., Vansteenkiste S., De Marre A. and Schacht E. (1995): *Glucose oxidase as a tool to study in vivo the interaction of glycosylated polymers with the mannose receptor of macrophages.* — J. Contr. Rel., Vol. 33, No. 1, pp. 115–123.

Gibaldi M. and Perrier D. (1975): *Pharmacokinetics.* — New York: Marcel Dekker.

Ibrir S. and Diop S. (2004): *A numerical procedure for filtering and efficient high-order signal differentiation.* — Int. J. Appl. Math. Comput. Sci., Vol. 14, No. 2, pp. 201–208.

Ljung L. and Glad T. (1994): *On global identifiability for arbitrary model parametrizations.* — Automatica, Vol. 30, No. 2, pp. 265–276.

Marino R. and Tomei P. (1995): *Adaptive observers with arbitrary exponential rate of convergence for nonlinear systems.* — IEEE Trans. Automat. Contr., Vol. 40, No. 7, pp. 1300–1304.

Roseeuw E., Coessens V., Balazuc A.-M., Lagranderie M., Chavarot P., Pessina A., Neri M.G., Schacht E., Marchal G. and Domurado D. (2003): *Synthesis, degradation and antimicrobial properties of targeted macromolecular prodrugs of norfloxacin.* — Antimicrob. Agents Chemother., Vol. 47, No. 11, pp. 3435–3441.

Vajda S., Godfrey K.R. and Rabitz H. (1989): *Similarity transformation approach to structural identifiability of nonlinear models.* — Math. Biosci., Vol. 93, pp. 217–248.

## Appendix

The aim of this appendix is to clarify the “technical assumptions” about the differential polynomials of  $\mathcal{C}_\theta$  that are given in the identifiability algorithm.

Let us begin by introducing the appropriate notation:

- $\mathcal{I}$  is the radical of the differential ideal generated by (5).
- $\mathcal{C}$  is a characteristic presentation of  $\mathcal{I}$  endowed with the ranking  $[\theta] \prec [y] \prec [x]$ ,

$$\mathcal{C} = \{\dot{\theta}_1, \dots, \dot{\theta}_p, P(y, \theta), Q_1(x, y, \theta), \dots, Q_n(x, y, \theta)\}.$$

- $\mathcal{L}$  is the set of the leaders of  $\mathcal{C}$ , i.e.,

$$\mathcal{L} = \{\dot{\theta}_1, \dots, \dot{\theta}_p, y^{(d)}, x_1^{(d_1)}, \dots, x_n^{(d_n)}\},$$

where  $\{d, d_1, \dots, d_n\}$  depend on the model.

- $\mathcal{N}$  is the set of the other derivatives occurring in  $\mathcal{C}$ , and  $\mathbb{R}[\mathcal{N}]$  is the polynomial ring built over  $\mathcal{N}$  with coefficients in  $\mathbb{R}$ .
- $\mathcal{C}(\theta)$  is the characteristic presentation  $\mathcal{C}$  evaluated at  $\theta$ , a particular parameter value.
- $\mathcal{I}_\theta$  is the radical of the differential ideal generated by (5) via considering  $\theta$ , a particular parameter value, and  $\mathcal{C}_\theta$  is the characteristic presentation of  $\mathcal{I}_\theta$ , endowed with the ranking  $[y] \prec [x]$ ,

In order to avoid the evaluation of  $\mathcal{C}(\theta)$  at each parameter value, the following result (Denis-Vidal et al., 2001b) gives a sufficient condition for the equality  $\mathcal{C}_\theta = \mathcal{C}(\theta)$ :

**Proposition A.** *Let  $\mathcal{C} = \{\dot{\theta}_1, \dots, \dot{\theta}_p, c_1, c_2, \dots, c_{n+1}\}$  be the characteristic presentation of the differential ideal  $\mathcal{I}$  endowed with the ranking  $[\theta] \prec [y] \prec [x]$ . If, for every  $\theta \in \mathcal{U}_p$  and for every  $i = 1, \dots, n + 1$ , the initial of  $c_i(\theta) \in \mathcal{C}(\theta)$  is nonzero and none of its factors ( $\neq 1$ ) is a divisor of all the other coefficients of  $c_i(\theta) \in \mathbb{R}[\mathcal{N}]$ , then  $\mathcal{C}_\theta = \mathcal{C}(\theta)$  for all  $\theta \in \mathcal{U}_p$ .*

The “technical assumptions” correspond to the assumptions of this proposition, which finally implies that the set  $\mathcal{C}_\theta^o = \mathcal{C}_\theta \cap \mathbb{R}(\theta)\{y\}$ , defined in Section 2.2, contains  $P(y, \theta)$ .

Let us illustrate this by the result of Step 3 applied to the model (1). The hypotheses of Proposition A are not valid if  $V_m k_c = 0$ . Indeed, the set  $\mathcal{L}$  is reduced to  $\mathcal{L} = \{\dot{y}\}$  and the input-output characteristic presentation can be rewritten as

$$\{(y + k_c)^2 \ddot{y} + T\},$$

where  $(y + k_c)^2$  and  $T$  belongs to  $\mathbb{R}[N]$ . If  $V_m = 0$ ,  $(y + k_c)^2$  is a divisor of  $T$  and  $k_c = 0$ , then  $y^2$  is a divisor of  $T$ .

Indeed, the software gives the result  $V_m k_c \neq 0$  directly, but this can be easily made explicit in the case of the model (1). In the same way, the result given by Step 3 applied to the model (2) can be checked.

Received: 20 December 2004  
 Revised: 19 July 2005  
 Re-revised: 15 September 2005